Network pharmacology and molecular docking reveal the mechanism of action of Bergapten against non-small cell lung cancer

YIHAO CHEN, YU FU, HONGBO ZOU, PINGSONG WANG, YAO XU and QICHAO XIE

Department of Oncology, The Third Affiliated Hospital of Chongqing Medical University, Chongqing 401120, P.R. China

Received June 10, 2024; Accepted October 28, 2024

DOI: 10.3892/ol.2024.14833

Abstract. Non-small cell lung cancer (NSCLC) is a leading cause of cancer mortality worldwide, necessitating new treatment approaches with minimal side effects. In the present study, the potential of Bergapten (5-methoxypsoralen), a natural furanocoumarin compound, as a therapeutic agent against NSCLC was investigated by using network pharmacology, molecular docking and *in vitro* validation. Bergapten targets were identified using the Traditional Chinese Medicine Systems Pharmacology Database and Analysis Platform and SwissTarget databases, whilst lung cancer-related targets were sourced from GeneCards and DisGeNET. Protein-protein interaction analysis and molecular docking were performed to identify key targets. The inhibitory effects of Bergapten on lung cancer cells were assessed using Cell Counting Kit-8 assays, wound healing assays, cell migration experiments, flow cytometry and western blotting. SC79 was used to verify the regulation of Bergapten on the PI3K/AKT pathway. Network pharmacology identified 51 targets, one signaling pathway and four Gene Ontology projects associated with the action of Bergapten against NSCLC. Key targets identified included glycogen synthase kinase-3β, Janus kinase 2, phosphatidylinositol-4,5-bisphosphate 3-kinase, catalytic subunit α and protein tyrosine kinase 2. *In vitro* experiments demonstrated that Bergapten significantly inhibited cell viability, promoted apoptosis, induced cellular senescence and inhibited the PI3K/AKT signaling pathway in NSCLC cells. In conclusion, Bergapten exerts its anti-NSCLC effects through the PI3K/AKT pathway, promoting cell senescence and inhibiting inflammation. These findings suggest that Bergapten has potential as a therapeutic agent for NSCLC.

Correspondence to: Professor Qichao Xie, Department of Oncology, The Third Affiliated Hospital of Chongqing Medical University, 1 Shuanghu Branch Road, Huixing Street, Yubei, Chongqing 401120, P.R. China
E-mail: 651072@cqmu.edu.cn

Key words: non-small cell lung cancer, 5-methoxypsoralen, PI3K/AKT, cell senescence

Introduction

Lung cancer (LC) is one of the most prevalent malignant tumors in humans, accounting for ~11.6% of all cancer cases worldwide, and remains the leading cause of cancer-related deaths, responsible for nearly 18.4% of total cancer mortality (1). The 5-year overall survival rate for LC is <20% (2,3). Based on pathological characteristics, LC is classified into two subtypes: Small cell lung cancer (SCLC) and non-small cell lung cancer (NSCLC) (1,4). NSCLC is particularly concerning due to its high invasiveness, malignancy and propensity to develop drug resistance, and accounts for ~85% of all LC cases and remains a leading cause of cancer mortality globally, contributing to ~125,000 deaths per year in the United States alone, as projected for 2024 (5). Therefore, there is an urgent need to identify effective anti-NSCLC therapies with minimal side effects.

Bergapten, also known as 5-methoxypsoralen, is a natural furanocoumarin that has garnered increasing attention for its medicinal potential. It exhibits a wide range of pharmacological effects, including neuroprotective, organ-protective, anticancer, anti-inflammatory, antibacterial and anti-diabetic properties (6).

Network pharmacology, based on systems biology theory, offers new strategies for investigating the relationship between drugs and diseases. It integrates systems biology, multidirectional pharmacobiology, bioinformatics and computer science. Network pharmacology has shifted biological system research from the traditional single-drug and single-target model to a multi-drug and multi-target approach (7). By constructing a 'component-protein/gene-disease' network, network pharmacology enables the high-throughput investigation of molecular regulatory mechanisms (8). These advantages make network pharmacology a powerful tool for studying combination therapies.

Given the urgent need to elucidate effective anti-NSCLC drugs with minimal side effects, the present study assessed Bergapten as a promising natural compound with potential anti-LC properties. The aim of this study was to evaluate the inhibitory effects of Bergapten on LC cell lines, particularly through its impact on the PI3K/AKT signaling pathway, which is crucial for cancer cell survival and proliferation (9). Additionally, the present study assessed whether Bergapten may promote cellular senescence in LC

cells, potentially limiting tumor progression through its pro-aging effects.

Materials and methods

Cell culture. NCI-H1975 (cat. no. iCell-h156), NCI-H1299 (cat. no. iCell-h153) and NCI-H460 (cat. no. iCell-h160) cells were purchased from iCell Bioscience Inc. and cultured in high-glucose medium (cat. no. PM00031, Proteintech Group, Inc.) supplemented with 10% fetal bovine serum (cat. no. F0850; Sigma-Aldrich; Merck KGaA) and 1% penicillin-streptomycin solution (Sigma-Aldrich; Merck KGaA) in a humidified atmosphere of 5% CO_2 at 37˚C. Cells were tested for mycoplasma contamination and all experiments were performed using cells from passages 3-5. Prior to specific treatments, cells were starved in serum-free medium for 1 h at 37˚C. Treatment with 5-methoxypsoralen and/or SC79 was performed for 12 h at 37˚C.

Reagents. The following reagents were used in the present study: 5-methoxypsoralen (cat. no. HY-N0370; MedChemExpress); RT Master Mix for qPCR II (gDNA digester plus; cat. no. HY-K0511A; MedChemExpress); Protein lysis solution (cat. no. P0013B; Beyotime Institute of Biotechnology); Cell Counting Kit-8 (CCK-8; cat. no. C0038; Beyotime Institute of Biotechnology); TRIzol™ (cat. no. 15596018; Invitrogen™; Thermo Fisher Scientific, Inc.); ChamQ Universal SYBR qPCR Master Mix (cat. no. Q711-02; Vazyme Biotech Co., Ltd.); fetal bovine serum (cat. no. F0850; Sigma-Aldrich; Merck KGaA); Phospho-AKT (Ser473) monoclonal antibodies (cat. no. 66444-1-Ig; Proteintech Group, Inc.); AKT monoclonal antibodies (cat. no. 60203-2-Ig; Proteintech Group, Inc.); PI3K p110 β polyclonal antibodies (cat. no. 20584-1-AP; Proteintech Group, Inc.); GAPDH monoclonal antibodies (cat. no. 60004-1-Ig; Proteintech Group, Inc.); Phospho-PI3K p85 (Tyr458)/p55 (Tyr199) antibodies (cat. no. 4228; CST Biological Reagents Co., Ltd.); RIPA Lysis Buffer (cat. no. P0013B; Beyotime Institute of Biotechnology); BeyoECL Plus (cat. no. P0018S; Beyotime Institute of Biotechnology); CCK-8 (cat. no. C0037; Beyotime Institute of Biotechnology); Annexin V-FITC Apoptosis Detection Kit (cat. no. C1062S; Beyotime Institute of Biotechnology); SC79 (25 mg; cat. no. SF2730; Beyotime Institute of Biotechnology); and Akt (pS473) + Total Akt ELISA Kit (cat. no. ab126433; Abcam).

Prediction of 5-methoxypsoralen target. The Traditional Chinese Medicine Systems Pharmacology Database and Analysis Platform (TCMSP) database (https://old.tcmsp-e.com/tcmsp.php) was searched using the keyword '5-methoxypsoralen' to identify its targets. Similarly, the SwissTarget database (http://www.swisstargetprediction.ch/) was queried to obtain additional targets for '5-methoxypsoralen'. The target names of 5-methoxypsoralen were converted into gene names using the UniProt database (https://www.uniprot.org/). After compiling the targets, duplicates were merged. Network and target prediction were conducted using the CytoHubba plug-in for Cytoscape software (version 3.7.2; Cytoscape Consortium; https://cytoscape.org/).

Prediction of potential targets for lung cancer. Using 'lung cancer' as the keyword, LC-related genes were retrieved from the GeneCards (https://www.genecards.org/) and DisGeNET (https://disgenet.com/) databases. After merging and removing duplicates, two independent operators performed the retrieval and summaries in separate rooms to minimize errors. The results were then reviewed by a third person for verification.

Obtaining common targets between 5-methoxypsoralen and LC. Using the online tool Venny 2.1.0 (https://bioinfogp.cnb.csic.es/tools/venny/), the potential targets of 5-methoxypsoralen and LC were uploaded and the intersection was taken to identify common 5-methoxypsoralen-LC targets. A Venn diagram was generated to illustrate the overlap.

To construct a protein-protein interaction (PPI) network, the common targets from the Venn diagram were imported into the Search Tool for the Retrieval of Interacting Genes/Proteins (STRING; https://string-db.org/) database, selecting 'multiple proteins' and setting the species to human. Targets were filtered with a confidence score of >0.7 and outliers were hidden. The TSV file was then downloaded and imported into Cytoscape to construct the PPI network and the '5-methoxypsoralen-shared target' network for anti-LC activity.

Gene ontology (GO) enrichment and Kyoto Encyclopedia of Genes and Genomes (KEGG) pathway enrichment. To perform enrichment analysis on the common targets of 5-methoxypsoralen and LC, the bioinformatics toolbar of the Xiantao academic website was used (https://www.xiantaozi.com/). The functional clustering option was selected and the common targets were uploaded. GO and KEGG enrichment functions available in the toolbar was used for the analysis.

Molecular docking verification. The structure of 5-methoxypsoralen was downloaded from the PubChem (https://pubchem.ncbi.nlm.nih.gov/) database. The downloaded file was then opened using PyMOL (v2.2.0 ;https://www.pymol.org/) and saved in PDB format for easier docking. The core target structure was obtained from the PDB database and opened in PyMOL. Water molecules and original ligands were deleted from the structure. Hydrogen atoms and charges were added to both the ligands and receptors to create a receptor grid. Molecular docking was performed using AutoDockVina 1.2.0 (10) and the binding strength between 5-methoxypsoralen and the receptor was evaluated based on the binding energy (Affinity, kcal/mol). PyMOL was used to visually display the conformation with the lowest binding energy.

Cell proliferation assay. The experiment consisted of three groups: The blank group, the experimental group and the negative control group. In the blank group, cells were cultured under normal conditions without any additional treatment, serving as a baseline for cell growth; in the experimental group, cells were treated with different concentrations of 5-methoxypsoralen; and in the negative control group, cells were cultured only with culture medium. NCI-H1975, H1299 and H460 cells were seeded at a density of $5x10^3$ cells/well in separate 96-well plates. After cell attachment, the cells were treated according to their respective groups for 72 h. Following the removal of the culture medium, CCK-8 solution was added

and the cells were incubated for 1 h. DMSO was then used to dissolve the crystals and absorbance was measured at 490 nm using a microplate reader. The cell survival rate was calculated as follows: (experimental group-negative control group)/(blank group-negative control group).

Reverse transcription-quantitative PCR (RT-qPCR) analysis. The experimental groups consisted of a control group and a 5-methoxypsoralen group. NCI-H1975, H1299 and H460 cells were individually seeded in 6-well plates at a density of $5x10^3$ cells/well. Once the cells adhered, the determined concentration of 5-methoxypsoralen from CCK-8 was added and the cells were treated for 72 h at 37˚C in a humidified atmosphere with 5% CO_2. Subsequently, TRIzol® reagent was used to extract the RNA from the cells. The extracted RNA was reverse-transcribed into cDNA using a commercial RT Master Mix for qPCR II kit (gDNA digester plus; MedChemExpress). The reverse transcription conditions were as follows: 25˚C for 5 min, 55˚C for 15 min and 85˚C for 2 min. For quantitative PCR, ChamQ Universal SYBR qPCR Master Mix (cat. no. Q711-02; Vazyme Biotech Co., Ltd.) was used, containing SYBR Green I dye as the fluorophore. The reaction mixture included 1 μg of RNA as template, along with the provided buffer and dNTPs. The thermocycling protocol was set as follows: 5˚C for 30 sec, then 95˚C for 10 sec and 60˚C for 30 sec for 40 cycles. The $2^{-\Delta\Delta Cq}$ method (11) was used to determine the relative expression of the targeted genes, with *Gapdh* mRNA serving as the internal reference. The primers used for RT-qPCR are listed in Table SI.

AKT phosphorylation assay. The effect of 5-methoxypsoralen was evaluated by measuring AKT phosphorylation stimulated by SC79 (Akt activator) in cells. Briefly, NCI-H1975, H1299 and H460 cells $3x10^3$ cells/well were starved for 1 h and 50% of the cells were collected to measure the basal level of AKT phosphorylation. After cells were treated with 50 μM 5-methoxypsoralen and/or 4 μg/ml SC79 for 12 h at 37˚C in a humidified atmosphere with 5% CO_2, the remaining 50% of the cells were collected. Phosphorylation of AKT was measured using an AKT ELISA kit.

Flow cytometry analysis. For cell apoptosis analyses, samples were analyzed using a BD FACSCanto II flow cytometer (BD Biosciences). Data were collected and processed using BD FACSDiva software (v8.0.1; BD Biosciences; https://www.bdbiosciences.com/en-us/products/software/instrument-software/bd-facsdiva-software). A total of $3x10^5$ NCI-H1975, H1299 and H460 cells were starved in serum-free medium for 12 h, followed by incubation with 5-methoxypsoralen in fresh serum-containing medium to promote cell cycle progression for 72 h at 37˚C in a humidified atmosphere with 5% CO_2. The cells were then collected and fixed with 1 ml ice-cold 70% ethanol and incubated at -20˚C for 24 h. Subsequently, the cells were centrifuged at 380 x g for 5 min at room temperature. Cell apoptosis was evaluated using the Annexin V-FITC Apoptosis Detection Kit.

Wound healing assay. A total of $3x10^5$ NCI-H1975, H1299 and H460 cells were cultured in 6-well tissue culture plates until they reached 100% confluency at 37˚C in a humidified atmosphere with 5% CO_2. Subsequently, they were incubated in starvation media containing 0.1% FBS for a period of 12 h at 37˚C in a humidified atmosphere with 5% CO_2. The monolayer of cells was then gently scraped using sterile 200 μl pipette tips. Images were captured using an Olympus CKX53 inverted microscope (Olympus Corporation) at two migration points, initially and after 24 h of the assay. The gap distances at 0 and 24 h after the wound were measured, and the migration efficiency was calculated as the difference between the gap area at 0 and 24 h.

Migration assay. For the migration and invasion assays, NCI-H1975, H1299 and H460 cells in the logarithmic growth phase were suspended in serum-free medium and seeded at a density of $3x10^5$ cells/well into the upper chamber of a Transwell insert (8 μm pore size; Corning Inc.). The lower chamber contained 600 μl culture medium with 20% fetal bovine serum, serving as a chemoattractant. Following a 24-h incubation at 37˚C in a humidified atmosphere with 5% CO_2, non-migrated cells on the upper surface of the insert were gently removed. Cells that had migrated or invaded to the lower surface were fixed with 4% paraformaldehyde at room temperature for 15 min, stained with crystal violet at room temperature for 5 min and imaged using an Olympus CKX53 inverted microscope (Olympus Corporation). Cell counts were performed from at least three random fields per insert to quantify migration and invasion.

Western blotting. A total of $3x10^5$ NCI-H1975, H1299 and H460 cells were seeded in 6-well plates and treated with 5-methoxypsoralen for 72 h at 37˚C in a humidified atmosphere with 5% CO_2. Subsequently, the cells were lysed using the RIPA lysis kit and the total protein quantification of whole cell lysates was performed using the BCA protein assay kit (Takara Biotechnology Co., Ltd.). Equal amounts of 30 μg protein were separated on a 10-12% SDS-PAGE gel and then electrophoretically transferred to a PVDF membrane. The membranes were blocked with 5% non-fat dry milk (cat. no. sc-2324; Santa Cruz Biotechnology, Inc.) in TBST (Tris-buffered saline with 0.1% Tween-20) for 1 h at room temperature to prevent non-specific binding. After blocking, primary antibodies were then applied and incubated overnight at 4˚C, including: Phospho-AKT (Ser473; 1:1,000; cat. no. 66444-1-Ig; Proteintech Group, Inc.), total AKT (1:1,000; cat. no. 60203-2-Ig; Proteintech Group, Inc.) and GAPDH (1:1,000; cat. no. 60004-1-Ig; Proteintech Group, Inc.), used as a loading control. The following secondary antibodies were used at a 1:5,000 dilution: Anti-rabbit IgG, HRP-conjugated (cat. no. SA00001-2; Proteintech Group, Inc.) and anti-mouse IgG, HRP-conjugated (cat. no. SA00001-1; Proteintech Group, Inc.). After a 1-h incubation with the secondary antibodies at room temperature, the membranes were washed and visualized using BeyoECL Plus chemiluminescent substrate (cat. no.P0018S; Beyotime Institute of Biotechnology), and the grayscale values of the protein bands were analyzed using Image J 1.0 software (https://imagej.net/ij/download.html).

Statistical analysis. Prism software v.9.0 (Dotmatics) was used for statistical analysis. Values are presented as mean ± standard deviation. The experiments in the presents

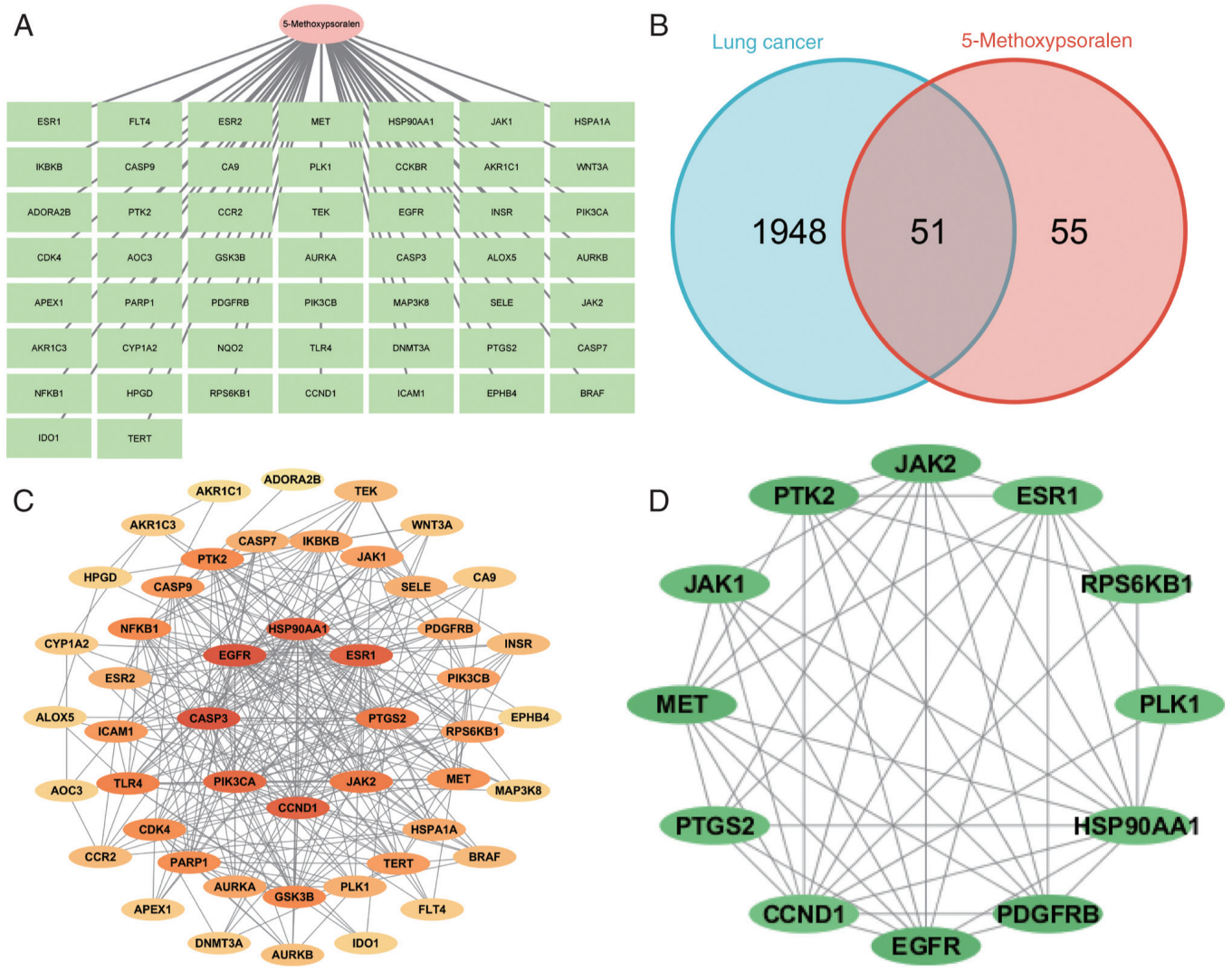

Figure 1. Drugs-potential targets network. (A) Network diagram of '5-methoxypsoralen-target'. (B) Venn diagram. (C) Network diagram of PPI of 5-methoxypsoralen against lung cancer. (D) Top 12 hub genes in PPI network. PPI, protein-protein interaction.

study were repeated ≥3 times independently. Comparisons between two groups were performed using two-tailed Student's t test and comparisons between multiple groups were performed using one-way ANOVA, followed by the Bonferroni test. $P<0.05$ were considered to indicate a statistically significant difference.

Results

Network pharmacology combined with molecular docking to explore the mechanism of 5-methoxypsoralen in the treatment of LC. The TCMSP database was used to search for Chinese medicine containing Bergapten (referred to as 'bergamot') by entering its name in the 'Herb name' column. The search yielded bergamot lactone with Mol ID MOL001945. The target names of 5-methoxypsoralen were converted into gene names using the UniProt database. The PubChem database provided the Canonical SMILES for bergapten, which was then entered into the SwissTarget database to predict its targets. The resulting targets were summarized and duplicates were removed (Fig. 1A).

To obtain LC-related targets, the GeneCards and DisGeNET databases were used. After integration and removal of duplicates, 1,948 target proteins associated with LC were identified. The Venny 2.1.0 tool was used to map the targets of 5-methoxypsoralen and LC, resulting in a Venn diagram and identifying 51 shared targets for the treatment of LC with 5-methoxypsoralen (Fig. 1B). These 51 shared targets were further analyzed using the STRING database, and the results were visualized and adjusted using Cytoscape 3.7.2 software. By hiding single nodes, a PPI network diagram of the shared targets was created (Fig. 1C). The color intensity of the targets indicates the strength of protein interactions, with heat shock protein 90 α family class A member 1 (HSP90AA1), Caspase 3 (CASP3), EGFR, AKT serine/threonine kinase 1 (AKT1) and prostaglandin-endoperoxide synthase 2 (PTGS2) nodes exhibiting markedly higher degree values compared with other nodes, suggesting that these are key targets of 5-methoxypsoralen in its anti-LC activity. The CytoHubba plug-in in Cytoscape was used to identify the hub genes in the PPI network diagram (Fig. 1D).

Table I. Gene Ontology and Kyoto Encyclopedia of Genes and Genomes analysis of potential targets.

Ontology	ID	Description	GeneRatio	BgRatio	P-value	P.adjust
BP	GO:0032355	Response to estradiol	10/51	123/18800	1.01×10^{-12}	2.65×10^{-9}
BP	GO:0018209	Peptidyl-serine modification	13/51	338/18800	4.2×10^{-12}	5.52×10^{-09}
BP	GO:1901653	Cellular response to peptide	13/51	361/18800	9.6×10^{-12}	8.41×10^{-9}
BP	GO:0046777	Protein autophosphorylation	11/51	224/18800	1.68×10^{-11}	1.06×10^{-8}
BP	GO:0033674	Positive regulation of kinase activity	14/51	476/18800	2.02×10^{-11}	1.06×10^{-8}
CC	GO:0045121	Membrane raft	9/51	326/19594	1.44×10^{-7}	1.24×10^{-5}
CC	GO:0098857	Membrane microdomain	9/51	327/19594	1.48×10^{-7}	1.24×10^{-5}
CC	GO:0061695	Transferase complex, transferring phosphorus-containing groups	7/51	259/19594	4.58×10^{-6}	0.0003
CC	GO:0005925	Focal adhesion	8/51	419/19594	1.16×10^{-5}	0.0005
CC	GO:0030055	Cell-substrate junction	8/51	428/19594	1.36×10^{-5}	0.0005
MF	GO:0004712	Protein serine/threonine/tyrosine kinase activity	20/51	446/18410	1.23×10^{-19}	3.36×10^{-17}
MF	GO:0004713	Protein tyrosine kinase activity	10/51	135/18410	3.17×10^{-12}	4.32×10^{-10}
MF	GO:0004714	Transmembrane receptor protein tyrosine kinase activity	7/51	60/18410	2.82×10^{-10}	2.55×10^{-8}
MF	GO:0019199	Transmembrane receptor protein kinase activity	7/51	79/18410	2.03×10^{-9}	1.38×10^{-7}
MF	GO:0043560	Insulin receptor substrate binding	4/51	10/18410	1.08×10^{-8}	5.89×10^{-7}
KEGG	hsa04151	PI3K-Akt signaling pathway	20/49	354/8164	2.91×10^{-15}	5.65×10^{-13}
KEGG	hsa05212	Pancreatic cancer	11/49	76/8164	4.72×10^{-13}	4.58×10^{-11}
KEGG	hsa05417	Lipid and atherosclerosis	15/49	215/8164	8.92×10^{-13}	5.77×10^{-11}
KEGG	hsa05215	Prostate cancer	11/49	97/8164	7.5×10^{-12}	3.64×10^{-10}
KEGG	hsa05162	Measles	12/49	139/8164	1.98×10^{-11}	7.69×10^{-10}

BP, biological process; GO, Gene Ontology; CC, cellular component; MF, molecular function; KEGG, Kyoto Encyclopedia of Genes and Genomes.

5-methoxypsoralen lactone is involved in multiple immune-related pathways and biological processes. To assess the biological processes and pathways of the potential targets, GO and KEGG analyses were performed using the Xiantao Academic platform. The results of the GO analysis and KEGG pathway enrichment ($P<0.05$) are presented in Table I. A total of 51 targets related to 5-methoxypsoralen were identified, which are primarily associated with the following biological processes: 'response to peptide', 'membrane raft', 'membrane microdomain', 'protein serine/threonine/tyrosine kinase activity' and the 'PI3K-Akt signaling pathway'.

Molecular docking and analysis. AutoDockVina was used to perform molecular docking and evaluate the binding affinity of bergamot lactone to eight key targets: CASP3, Cyclin D1 (CCND1), estrogen receptor 1 (ESR1), glycogen synthase kinase-3β (GSK3B), Janus kinase 2 (JAK2), NF-κB, phosphatidylinositol-4,5-bisphosphate 3-kinase, catalytic subunit α (PIK3CA), protein tyrosine kinase 2 (PTK2) and toll-like receptor 4 (TLR4). The ligand used for docking was 5-methoxypsoralen. The binding energies between 5-methoxypsoralen and the key targets were all found to be <-5.0 kcal/mol, indicating favorable binding affinities and suggesting these targets as potential candidates for 5-methoxypsoralen. Notably, the highest docking score (-7.9 kcal/mol) was observed between 5-methoxypsoralen and GSK3B, implying that GSK3B is a promising target for the anti-LC effects of 5-methoxypsoralen. The conformation with the lowest binding energy was visualized using PyMOL v2.2.0 (Fig. 2).

Effects of 5-methoxypsoralen on cell viability and apoptosis of NCI-H1975, NCI-H1299 and NCI-H460. The cytotoxic effect of 5-methoxypsoralen on NCI-H1975, H1299 and H460 cells was assessed using the CCK-8 assay. Treatment with 40 μM 5-methoxypsoralen for 72 h significantly reduced cell viability in NCI-H1975 and H1299 cells compared with untreated control cells (Fig. 3A). Similarly, treatment with 50 μM 5-methoxypsoralen for 72 h significantly inhibited cell viability in NCI-H460 cells relative to the untreated control group. Therefore, these concentrations were selected for further experiments. Additionally, the effect of 5-methoxypsoralen on apoptosis in LC cells was evaluated (Fig. 3B) and the results indicated that 5-methoxypsoralen treatment promoted apoptosis in all three types of LC cell. In conclusion, these findings suggest that 5-methoxypsoralen exhibits significant cytotoxic effects on NCI-H1975, NCI-H1299 and NCI-H460 cells.

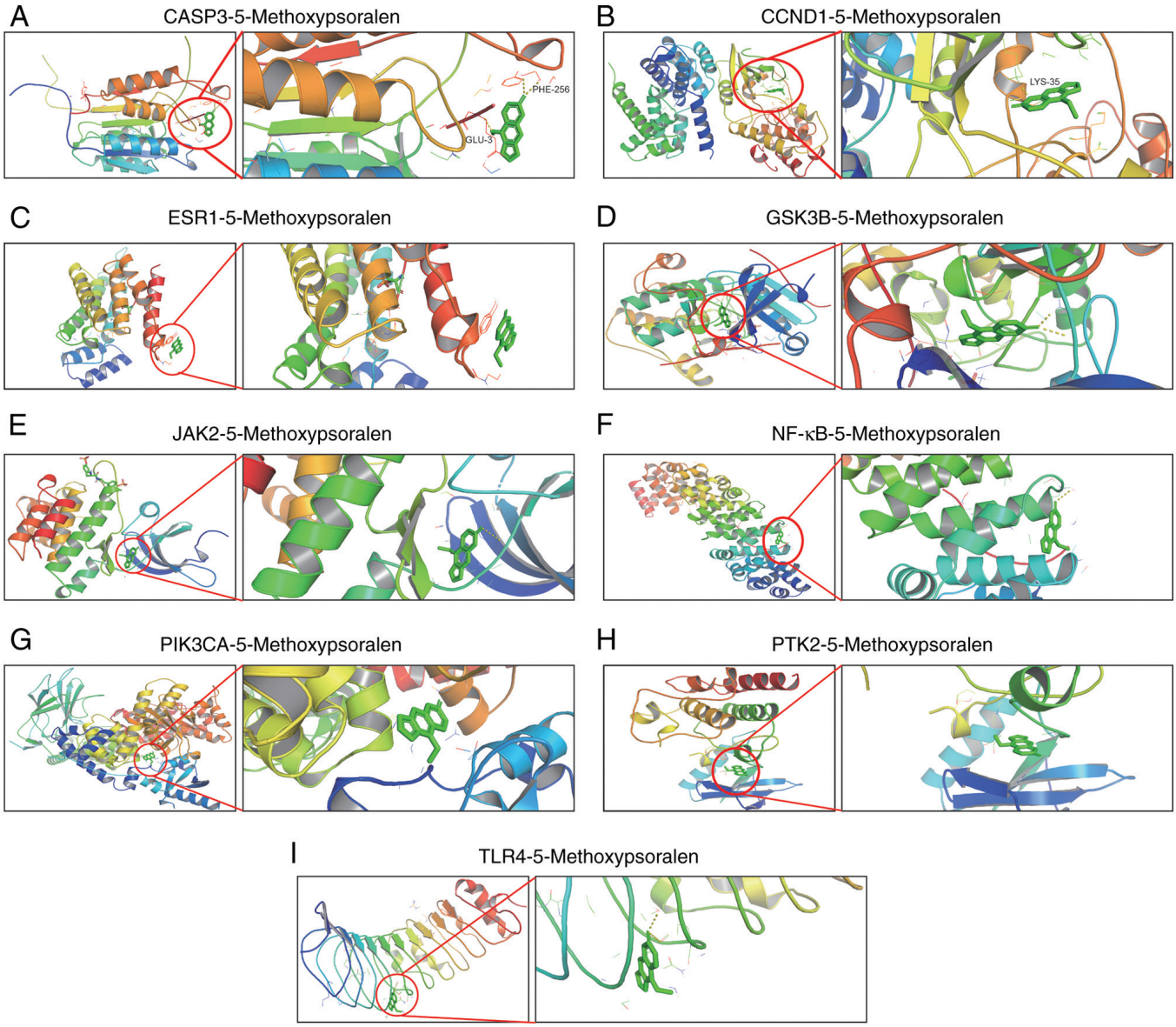

Figure 2. Molecular model of 5-methoxypsoralen binding to its predicted protein target. Proteins (A) CASP3, (B) CCND1, (C) ESR1, (D) GSK3B, (E) JAK2, (F) NF-κB, (G) PIK3CA, (H) PTK2 and (I) TLR4 were demonstrated to be associated with 5-methoxypsoralen interactions, represented by the blue stick model. Lines represent residues in the binding site. The light dashed lines represent hydrogen bonds and the dark dashed lines demarcate π-π interactions. CASP3, Caspase 3; CCND1, Cyclin D1; ESR1, estrogen receptor 1; GSK3B, glycogen synthase kinase-3β; JAK2, Janus kinase 2; PIK3CA, phosphatidylinositol-4,5-bisphosphate 3-kinase, catalytic subunit α; PTK2, protein tyrosine kinase 2; TLR4, toll-like receptor 4.

Molecular docking target protein verification. CASP3 is a classic indicator of apoptosis and CCND1 is a key driver of the malignant transformation of SCLC (12). Preclinical data support that ESR1 can stimulate NSCLC cell growth (13). GSK3B positive expression in LC is associated with more advanced tumor stages and worse overall survival (14). Inhibition of JAK2 signaling can enhance radiotherapy in lung cancer models (15). Furthermore, although NF-κB has key physiological functions in normal cells (especially immune cells), specific inhibition of NF-κB in LC cells is crucial for alleviating inflammation and preventing LC. Blocking NF-κB promotes apoptosis in LC cells (16). High expression of PIK3CA is also associated with NSCLC in patients with a history of smoking (17). PTK2 is considered a novel therapeutic target for overcoming acquired EGFR-TKI resistance in NSCLC (18). Compared with non-LC tissues, TLR4 levels are higher in LC tissues and TLR4 helps LC cells evade the immune system by releasing immunosuppressive cytokines and enhancing resistance to pro-apoptotic factors (19).

In the present study, 50 μM 5-methoxypsoralen was used to evaluate the molecular docking results. The RT-qPCR experiments demonstrated that 5-methoxypsoralen significantly upregulated the expression of *CASP3* in the three LC cell lines and significantly inhibited the expression of *CCND1*, *ESR1*, *GSK3B*, *JAK2*, *NFKB*, *PIK3CA*, *PTK2* and *TLR4*, in comparison with controls (Fig. S1). These findings not only confirm the reliability of the molecular docking results but also suggest that 5-methoxypsoralen may have the potential to promote apoptosis, inhibit proliferation, and reduce immune escape in lung cancer cells.

5-methoxypsoralen inhibits the growth of LC cells in vitro. A wound healing assay was performed to measure cell migration,

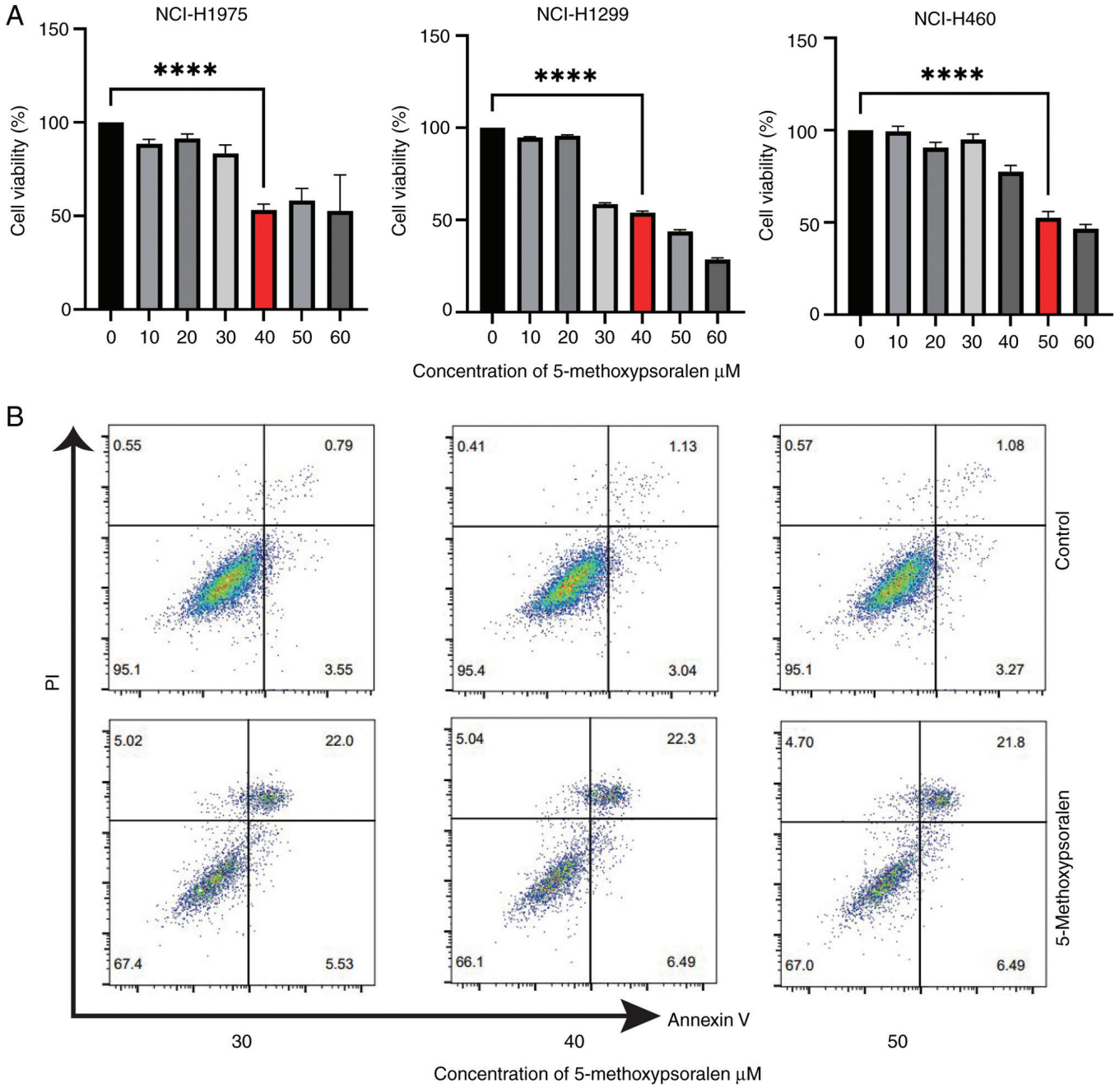

Figure 3. Effects of 5-methoxypsoralen on the viability and apoptosis levels of NCI-H1975, NCI-H1299 and NCI-H460 cells. (A) After 72 h of treatment with 5-methoxypsoralen, the viability of these cells was measured using the Cell Counting Kit-8 assay and the optimal drug concentration was determined. (B) Apoptosis levels was measured using flow cytometry after 72 h of treatment with 5-methoxypsoralen. n=3. ****P<0.0001.

where the distance between the edges of three cell monolayers (wound width) was measured after 24 h of treatment with 5-methoxypsoralen. The results indicated that 5-methoxypsoralen at concentrations of 40 or 50 μM significantly reduced the migration of LC cells, in comparison with controls (Fig. 4). Additionally, the migration of LC cells was evaluated using a Transwell assay. The findings demonstrated that 5-methoxypsoralen at concentrations of 40 or 50 μM significantly inhibited the migration ability of LC cells compared with controls, particularly in NCI-H1299 cells (Fig. 5).

5-methoxypsoralen inhibits the PI3K/AKT pathway in lung cancer cells and promotes cellular senescence. The KEGG results indicated that 5-methoxypsoralen may impact the PI3K/AKT pathway in LC, which was subsequently evaluated *in vitro*. The results demonstrated a significant reduction in the expression of P-PI3K and P-AKT in the 5-methoxypsoralen group compared with the control group. However, no significant differences were observed in the expression of total AKT and PI3K between the groups (Fig. 6A and B).

During cellular senescence, several changes occur in DNA, proteins, secreted factors and cell morphology. This includes the secretion of a substantial amount of pro-inflammatory factors (20). RT-qPCR results revealed that treatment with 5-methoxypsoralen significantly activated the aging

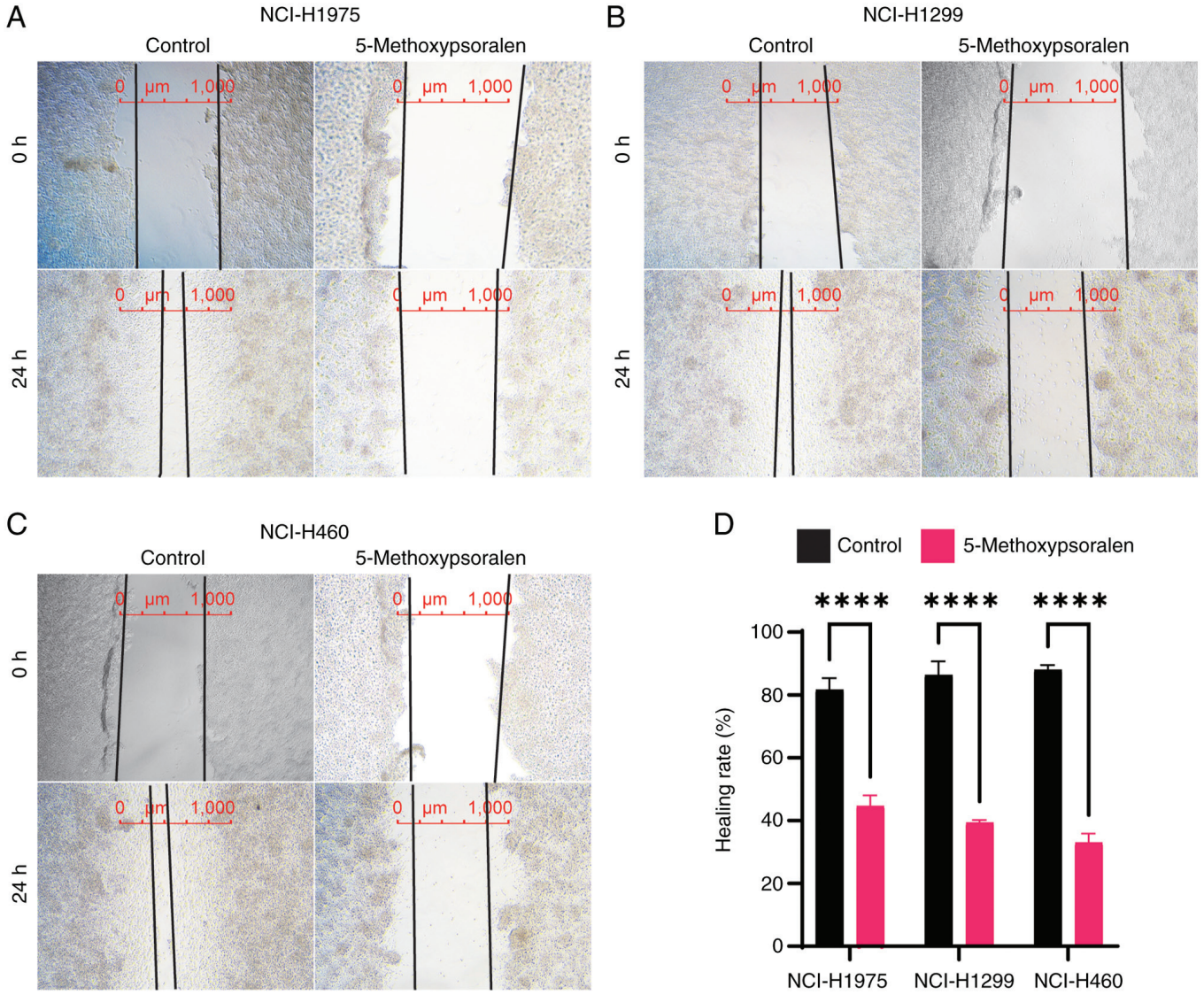

Figure 4. 5-methoxypsoralen inhibits the migration of lung cancer cells. Representative images of wound healing assays using 40 or 50 μM 5-methoxypsoralen in (A) NCI-H1975, (B) NCI-H1299 and (C) NCI-H460 cells (magnification, x200). (D) Quantification of migration efficiency in wound healing assay. n=3. ****P<0.0001.

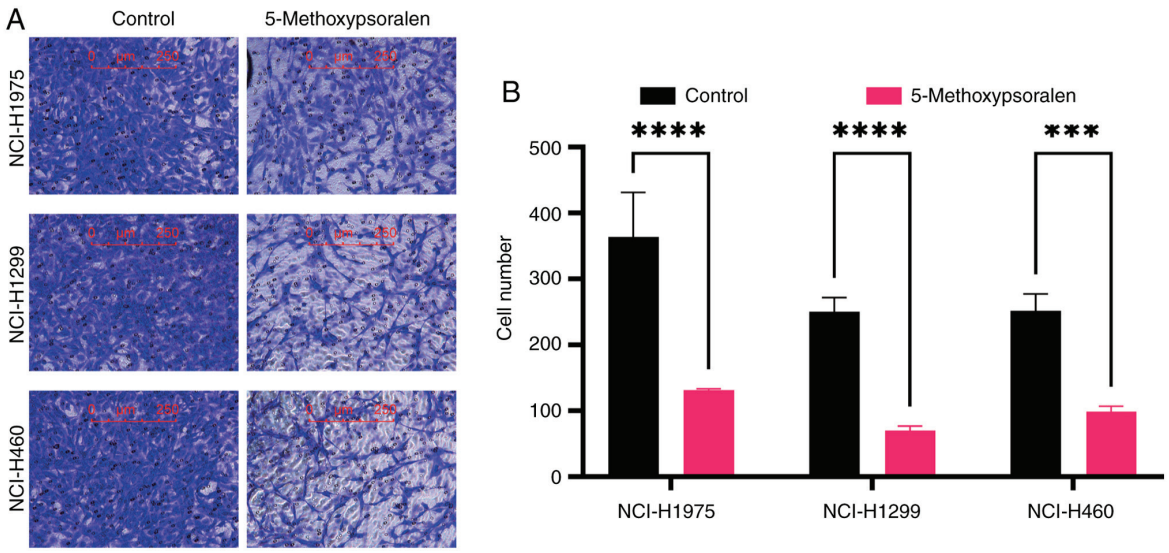

Figure 5. 5-methoxypsoralen inhibits the migration of lung cancer cells. (A) Representative images of NCI-H1975, NCI-H129 and NCI-H460 cells treated with 40 or 50 μM 5-methoxypsoralen (magnification, x200). (B) Fold change of migrated cell numbers. n=3. ***P<0.001; ****P<0.0001.

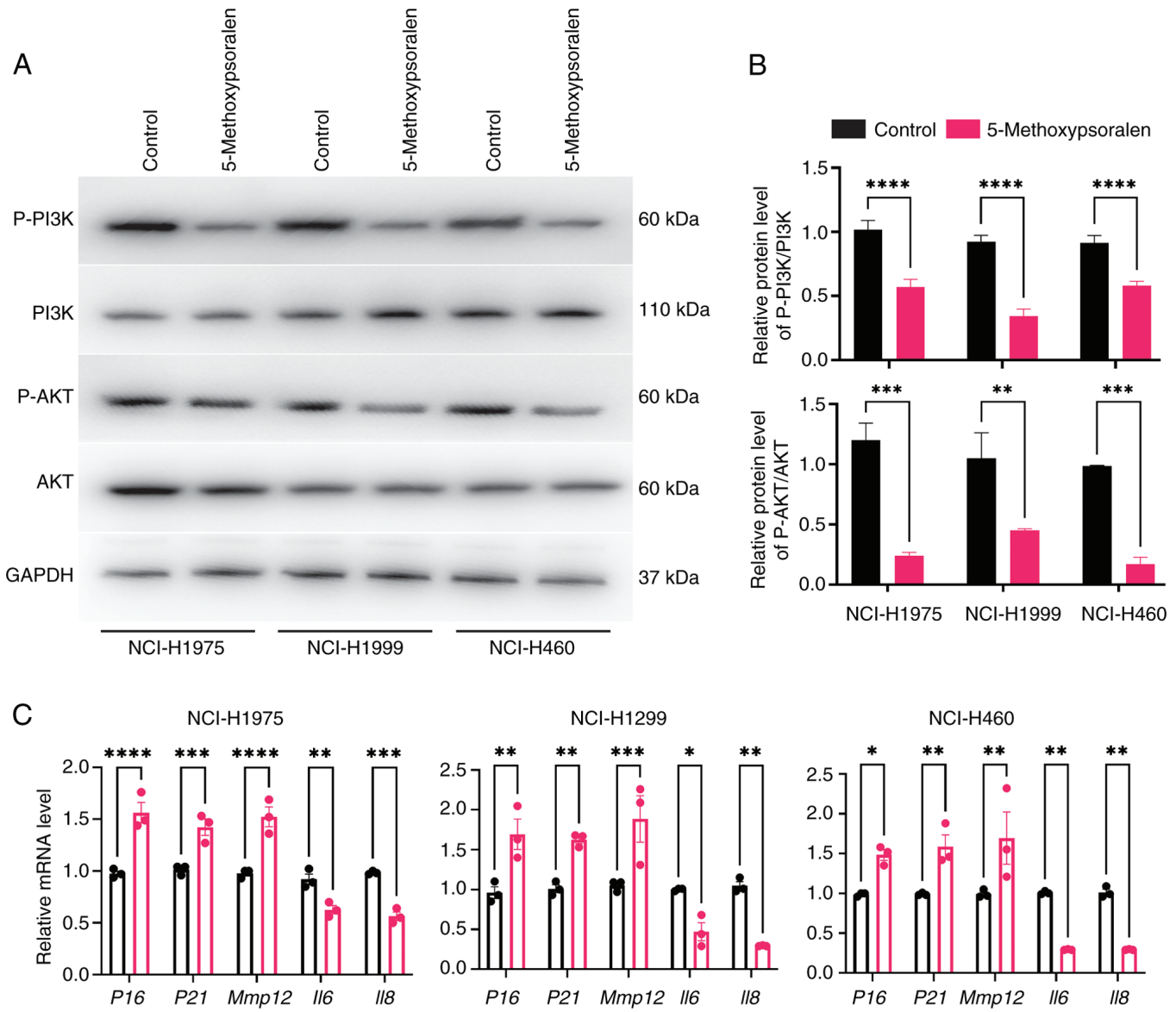

Figure 6. PI3K/AKT signaling pathway and pro-aging serve important roles in the inhibitory effect of 5-methoxypsoralen on non-small cell lung cancer. (A) Western blot analysis used to determine the expression of P-PI3K, PI3K, P-AKT and AKT proteins in three types of cells after treatment 5-methoxypsoralen. (B) Quantification of western blot analysis in three types of cells after treatment 5-methoxypsoralen. (C) RT-qPCR analysis determined the *P16*, *P21*, *MMP12*, *IL6* and *IL8* mRNA levels after treatment with 5-methoxypsoralen. n=3. *P<0.05, **P<0.01; ***P<0.001; ****P<0.0001.

markers *P16* and *P21*, in comparison with the control group. Additionally, 5-methoxypsoralen treatment also influenced senescence-associated secretory phenotype (SASP), with increased expression of *MMP12* and decreased levels of *IL6* and *IL8* (Fig. 6C).

AKT activator SC79 attenuates the negative effects of 5-methoxypsoralen on LC cells. To further assess whether the regulatory effect of 5-methoxypsoralen on cells depends on the PI3K/AKT pathway, SC79, an AKT activator, for verification. SC79 is known for its high safety profile and ability to activate multiple phosphorylation sites of AKT. Even after SC79 is removed, sustained increases in Akt phosphorylation levels can be observed both in cell cultures and *in vivo* (21).

In the present study, AKT activity significantly increased in all three cell types following treatment with SC79, compared with the 5-methoxypsoralen group (Fig. 7A). Subsequently, the effect of SC79 on cell apoptosis was evaluated. The results revealed that SC79 treatment, after 5-methoxypsoralen exposure, significantly reduced the mRNA levels of apoptotic markers *CASP3, 7* and *9* in comparison with the 5-methoxypsoralen group (Fig. 7B), suggesting that AKT activation inhibits cell apoptosis and that 5-methoxypsoralen exerts its pro-apoptotic effect through AKT.

Additionally, the impact of SC79 on SASP was assessed. Following combined treatment with SC79 and 5-methoxypsoralen, the mRNA levels of *P16*, *P21* and *MMP12* decreased, whilst the mRNA levels of *IL6* and *IL8* increased in comparison with the 5-methoxypsoralen group (Fig. 7C). These findings suggest that the ability of 5-methoxypsoralen to promote tumor cell senescence and inhibit inflammation is also dependent on AKT activity.

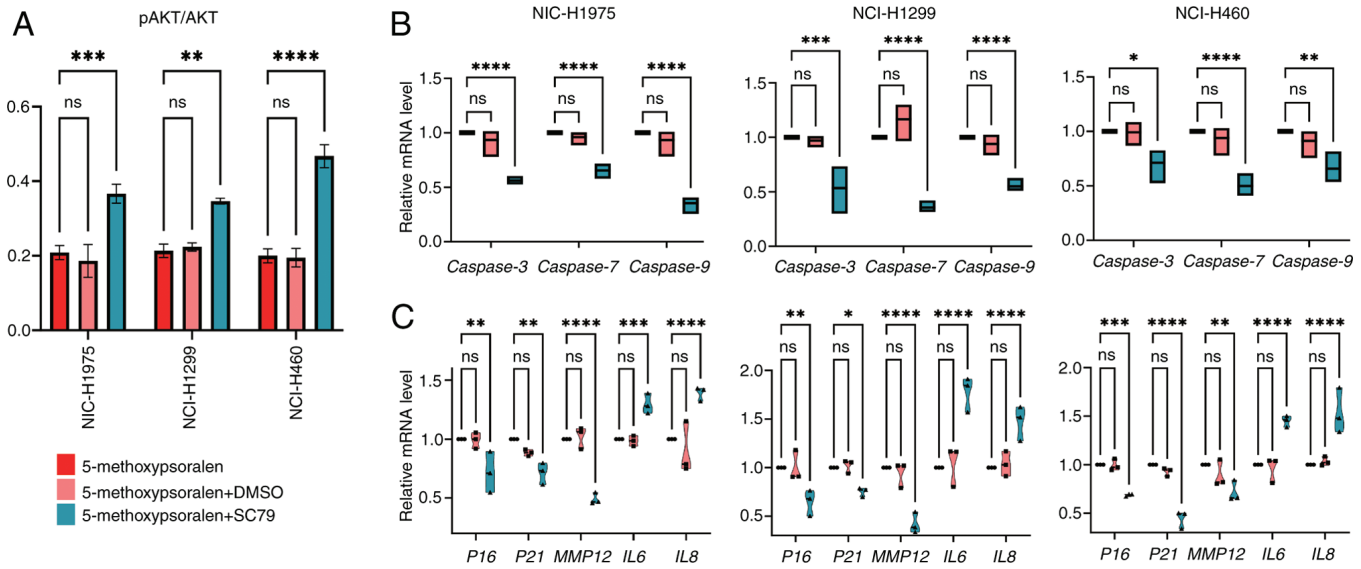

Figure 7. SC79 (4 μg/ml) antagonizes the negative effects of 5-methoxypsoralen on non-small cell lung cancer. (A) ELISA was used to detect the AKT activation levels of three cell lines after treatment with 5-methoxypsoralen, 5-methoxypsoralen + DMSO and 5-methoxypsoralen + SC79. (B) RT-qPCR analysis determined the *Caspase3*, *7* and *9* mRNA levels after treatment with 5-methoxypsoralen, 5-methoxypsoralen + DMSO and 5-methoxypsoralen + C79. (C) RT-qPCR analysis determined the *P16*, *P21*, *MMP12*, *IL6* and *IL8* mRNA levels after treatment with 5-methoxypsoralen, 5-methoxypsoralen + DMSO and 5-methoxypsoralen + SC79. n=3. *P<0.05; **P<0.01; ***P<0.001; ****P<0.0001. RT-qPCR, reverse transcription-quantitative PCR; MMP12, matrix metallopeptidase 12; ns, no significant difference.

Discussion

The present study assessed the anticancer effects of 5-methoxypsoralen on the human LC cell lines, NCI-H1975, H1299 and H460. The results demonstrated that 5-methoxypsoralen effectively inhibited the viability of these cell types, attributed to its ability to induce apoptosis and senescence, as well as its inhibition of the PI3K/AKT signaling pathway. Network pharmacology analysis revealed that 5-methoxypsoralen may exert its anti-LC effects primarily by targeting HSP90AA1, CASP3, EGFR, AKT1, GSK3B and PTGS2. Molecular docking results showed strong binding between Bergapten (5-methoxypsoralen) and these targets, with the highest binding affinity observed for GSK3B. This suggests that 5-methoxypsoralen exerts its anti-LC effects by modulating GSK3B and its associated pathways.

The KEGG enrichment analysis results revealed that 5-methoxypsoralen may have a therapeutic effect on LC through the PI3K-AKT signaling pathway (Table I). The PI3K-AKT signaling pathway is known to be involved in cell growth, survival and metabolism (22). Previous studies have demonstrated that this pathway interacts with DNA damage response, which is a key factor in aging (23). The activation of PI3K cascade leads to the activation of downstream survival molecules, such as AKT (24). The PI3K/AKT pathway serves a crucial role in regulating cell growth, motility and survival during the progression and metastasis of cancer; it is frequently activated in cancer cells. Furthermore, activation of the AKT signaling pathway results in resistance to apoptosis, including the inactivation of anti-apoptotic genes and pro-apoptotic factors (25).

There is increasing evidence linking cellular senescence and inflammation. Cellular senescence is a natural and unavoidable process in organisms, resulting in permanent cell cycle arrest (26,27). Whilst aging is associated with several diseases, senescent cells can also have a positive role. In cancer, aging acts as an effective barrier against tumorigenesis (28). A characteristic of senescent cells is the elevated activity of lysosomal β-galactosidase. Senescent cells secrete pro-inflammatory factors such as IL-6, TNF-α and matrix metallopeptidase 12 (MMP12), known as the SASP, which can induce physiological changes in the surrounding environment, including inflammation, tumor formation and growth arrest. Studies have demonstrated that certain SASP factors, like IL-1β, can induce senescence in normal cells, whilst IL-6 can further accelerate the senescence process in senescent cells. The loss of IL-6 can disrupt the inflammation-related SASP network and the aging paracrine pathway (29). There has been a rise in studies focusing on the senescence of LC cells. *In vitro*, A549 cells irradiated with a single high dose exhibit SASP (30). Moreover, knockdown of MMP12 inhibits the growth and migration of lung adenocarcinoma cells (31).

The present study aimed to evaluate the effects of 5-methoxypsoralen on senescence and SASP in LC cell lines. The results from RT-qPCR analysis indicated that 5-methoxypsoralen can induce senescence in LC cells. Whilst both *IL6* and *IL8* are part of SASP, they serve different roles in LC. IL-6 is known to promote NSCLC metastasis by upregulating T-cell immunoglobulin domain and mucin domain 4 (TIM-4) (32), whereas reducing IL-8 secretion inhibits LC metastasis to the brain (33). Notably, 5-methoxypsoralen was reported to inhibit the levels of *IL6* and *IL8* in LC cell lines, suggesting that it not only promotes senescence in LC cells but also inhibits chronic inflammation in the cancer micro-environment, thereby limiting tumor progression. Moreover, the present study demonstrated that the regulation of 5-methoxypsoralen on LC cell lines was significantly

impeded after the use of the AKT activator SC79, which also suggests that 5-methoxypsoralen does exert its anticancer effect *in vitro* through PI3K/AKT.

The case report by Hashimoto *et al* (34) highlights the clinical challenges posed by metastatic lung adenocarcinoma, including the aggressiveness and resilience of metastatic cells. Understanding how Bergapten and similar compounds affect metastatic lesions could provide critical insights into their broader therapeutic potential, particularly in preventing or treating metastasis in patients with LC.

To fully understand the therapeutic potential of Bergapten, it is critical to bridge the gap between *in vitro* concentrations and achievable *in vivo* plasma concentrations in humans. Whilst the *in vitro* results of the present study are promising, demonstrating significant effects on cancer cell viability, apoptosis and pathway modulation, the concentrations used may not be directly translatable to clinical settings without considering factors like bioavailability, delivery methods and potential toxicity. Therefore, further pharmacokinetic studies and *in vivo* experiments are needed to determine the clinical feasibility of using Bergapten as an anticancer agent and to optimize its delivery to achieve therapeutic concentrations at the target site.

The present study on the effect of Bergapten on NSCLC has advantages and limitations. Network pharmacology was used to predict the key targets and pathways involved in the anticancer effect of Bergapten, which was further assessed *in vitro*. The strong binding affinity of Bergapten to key proteins was confirmed by molecular docking, which enhanced the understanding of its mechanism of action. However, the results of the present study are based on *in vitro* assays and cannot fully replicate the complexity of organisms. Therefore, *in vivo* validation is required. In addition, the present study mainly targeted the PI3K/AKT pathway and did not assess other related pathways in the progression of NSCLC. For instance, mitochondrial deoxyguanosine kinase has been reported to markedly influence apoptosis and autophagy in lung adenocarcinoma cells (35), offering insights into the potential mechanisms through which Bergapten might exert its effects on cell viability and survival in NSCLC. The interplay between mitochondrial function and the PI3K/AKT pathway could further elucidate the mechanistic basis for the anticancer activity of Bergapten. In addition, the present study did not address the long-term safety and potential side effects of Bergapten; therefore, its clinical application needs further study.

In conclusion, the present study used network pharmacology and molecular docking technology to predict the potential anti-LC target of 5-methoxypsoralen and its mechanism of action. The combined experimental findings further support the notion that 5-methoxypsoralen may promote LC cell senescence and exert its pharmacological effects in treating LC by inhibiting the PI3K/AKT signaling pathway, regulating SASP and the micro-environment, and modulating the expression of *P16*/*P21* aging-related genes.

Acknowledgements

Not applicable.

Funding

The present work was supported by the Chongqing Science and Technology Bureau (grant no. cstc2019jcyj-msxmX0190).

Availability of data and materials

The data generated in the present study may be requested from the corresponding author.

Authors' contributions

YC conceived and designed the study with input from QX. YF performed the majority of the experiments and analyzed the data. HZ and PW assisted with data analysis and interpretation. YX conducted the cell viability and migration assays. YC and QX supervised the project. YC wrote the manuscript with contributions from all authors. All authors read and approved the final version of the manuscript. YC and QX confirm the authenticity of all the raw data.

Ethics approval and consent to participate

Not applicable.

Patient consent for publication

Not applicable.

Competing interests

The authors declare that they have no competing interests.

References

1. Bray F, Ferlay J, Soerjomataram I, Siegel RL, Torre LA and Jemal A: Global cancer statistics 2018: GLOBOCAN estimates of incidence and mortality worldwide for 36 cancers in 185 countries. CA Cancer J Clin 68: 394-424, 2018.
2. Pakzad R, Mohammadian-Hafshejani A, Ghoncheh M, Pakzad I and Salehiniya H: The incidence and mortality of lung cancer and their relationship to development in Asia. Transl Lung Cancer Res 4: 763-774, 2015.
3. Amini A, Byers LA, Welsh JW and Komaki RU: Progress in the management of limited-stage small cell lung cancer. Cancer 120: 790-798, 2014.
4. Liu Y, Ao X, Yu W, Zhang Y and Wang J: Biogenesis, functions, and clinical implications of circular RNAs in non-small cell lung cancer. Mol Ther Nucleic Acids 27: 50-72, 2021.
5. American Cancer Society: Cancer Facts & Figures 2024. https://www.cancer.org/research/cancer-facts-statistics/all-cancer-facts-figures/2024-cancer-facts-figures.html. Accessed October 22, 2024.
6. Liang Y, Xie L, Liu K, Cao Y, Dai X, Wang X, Lu J, Zhang X and Li X: Bergapten: A review of its pharmacology, pharmacokinetics, and toxicity. Phytother Res 35: 6131-6147, 2021.
7. Luo TT, Lu Y, Yan SK, Xiao X, Rong XL and Guo J: Network pharmacology in research of chinese medicine formula: Methodology, application and prospective. Chin J Integr Med 26: 72-80, 2020.
8. Zhou Z, Chen B, Chen S, Lin M, Chen Y, Jin S, Chen W and Zhang Y: Applications of network pharmacology in traditional Chinese medicine research. Evid Based Complement Alternat Med 2020: 1646905, 2020.
9. Peng Y, Wang Y, Zhou C, Mei W and Zeng C: PI3K/Akt/mTOR pathway and its role in cancer therapeutics: Are we making headway? Front Oncol 12: 819128, 2022.
10. Eberhardt J, Santos-Martins D, Tillack AF and Forli S: AutoDock Vina 1.2.0: New docking methods, expanded force field, and python bindings. J Chem Inf Model 61: 3891-3898, 2021.

11. Livak KJ and Schmittgen TD: Analysis of relative gene expression data using real-time quantitative PCR and the 2(-Delta Delta C(T)) method. Methods 25: 402-408, 2001.
12. Gautschi O, Ratschiller D, Gugger M, Betticher DC and Heighway J: Cyclin D1 in non-small cell lung cancer: A key driver of malignant transformation. Lung Cancer 55: 1-14, 2007.
13. Siegfried JM, Hershberger PA and Stabile LP: Estrogen receptor signaling in lung cancer. Semin Oncol 36: 524-531, 2009.
14. Alves M, Borges DP, Kimberly A, Martins Neto F, Oliveira AC, de Sousa JC, Nogueira CD, Carneiro BA and Tavora F: Glycogen synthase kinase-3 beta expression correlates with worse overall survival in non-small cell lung cancer-A clinicopathological series. Front Oncol 11: 621050, 2021.
15. Sun Y, Moretti L, Giacalone NJ, Schleicher S, Speirs CK, Carbone DP and Lu B: Inhibition of JAK2 signaling by TG101209 enhances radiotherapy in lung cancer models. J Thorac Oncol 6: 699-706, 2011.
16. Chen W, Li Z, Bai L and Lin Y: NF-kappaB in lung cancer, a carcinogenesis mediator and a prevention and therapy target. Front Biosci (Landmark Ed) 16: 1172-1185, 2011.
17. Wang Y, Wang Y, Li J, Li J and Che G: Clinical significance of PIK3CA gene in non-small-cell lung cancer: A systematic review and meta-analysis. Biomed Res Int 2020: 3608241, 2020.
18. Tong X, Tanino R, Sun R, Tsubata Y, Okimoto T, Takechi M and Isobe T: Protein tyrosine kinase 2: A novel therapeutic target to overcome acquired EGFR-TKI resistance in non-small cell lung cancer. Respir Res 20: 270, 2019.
19. Hoden B, DeRubeis D, Martinez-Moczygemba M, Ramos KS and Zhang D: Understanding the role of Toll-like receptors in lung cancer immunity and immunotherapy. Front Immunol 13: 1033483, 2022.
20. Payea MJ, Anerillas C, Tharakan R and Gorospe M: Translational control during cellular senescence. Mol Cell Biol 41: e00512-20, 2021.
21. Jo H, Mondal S, Tan D, Nagata E, Takizawa S, Sharma AK, Hou Q, Shanmugasundaram K, Prasad A, Tung JK, *et al*: Small molecule-induced cytosolic activation of protein kinase Akt rescues ischemia-elicited neuronal death. Proc Natl Acad Sci USA 109: 10581-10586, 2012.
22. Manning BD and Toker A: AKT/PKB signaling: Navigating the network. Cell 169: 381-405, 2017.
23. Maidarti M, Anderson RA and Telfer EE: Crosstalk between PTEN/PI3K/Akt signalling and DNA damage in the oocyte: Implications for primordial follicle activation, oocyte quality and ageing. Cells 9: 200, 2020.
24. Oh SJ, Erb HHH, Hobisch A, Santer FR and Culig Z: Sorafenib decreases proliferation and induces apoptosis of prostate cancer cells by inhibition of the androgen receptor and Akt signaling pathways. Endocr Relat Cancer 19: 305-319, 2012.
25. Reuter S, Eifes S, Dicato M, Aggarwal BB and Diederich M: Modulation of anti-apoptotic and survival pathways by curcumin as a strategy to induce apoptosis in cancer cells. Biochem Pharmacol 76: 1340-1351, 2008.
26. Kowald A, Passos JF and Kirkwood TBL: On the evolution of cellular senescence. Aging Cell 19: e13270, 2020.
27. Wiley CD and Campisi J: The metabolic roots of senescence: Mechanisms and opportunities for intervention. Nat Metab 3: 1290-1301, 2021.
28. Calcinotto A, Kohli J, Zagato E, Pellegrini L, Demaria M and Alimonti A: Cellular senescence: Aging, cancer, and injury. Physiol Rev 99: 1047-1078, 2019.
29. Salama R, Sadaie M, Hoare M and Narita M: Cellular senescence and its effector programs. Genes Dev 28: 99-114, 2014.
30. Tesei A, Arienti C, Bossi G, Santi S, De Santis I, Bevilacqua A, Zanoni M, Pignatta S, Cortesi M, Zamagni A, *et al*: TP53 drives abscopal effect by secretion of senescence-associated molecular signals in non-small cell lung cancer. J Exp Clin Cancer Res 40: 89, 2021.
31. Lv FZ, Wang JL, Wu Y, Chen HF and Shen XY: Knockdown of MMP12 inhibits the growth and invasion of lung adenocarcinoma cells. Int J Immunopathol Pharmacol 28: 77-84, 2015.
32. Liu C, Yang L, Xu H, Zheng S, Wang Z, Wang S, Yang Y, Zhang S, Feng X, Sun N, *et al*: Systematic analysis of IL-6 as a predictive biomarker and desensitizer of immunotherapy responses in patients with non-small cell lung cancer. BMC Med 20: 187, 2022.
33. Li C, Zheng H, Xiong J, Huang Y, Li H, Jin H, Ai S, Wang Y, Su T, Sun G, *et al*: miR-596-3p suppresses brain metastasis of non-small cell lung cancer by modulating YAP1 and IL-8. Cell Death Dis 13: 699, 2022.
34. Hashimoto K, Nishimura S and Akagi M: Lung adenocarcinoma presenting as a soft tissue metastasis to the shoulder: A case report. Medicina (Kaunas) 57: 181, 2021.
35. Liu C, Qin Q and Cong H: Research progress on the relationship between mitochondrial deoxyguanosine kinase and apoptosis and autophagy in lung adenocarcinoma cells. Cancer Insight 1: 53-62, 2022.